Front. Chem. Sci. Eng. 2020, 14(1): 97–104
https://doi.org/10.1007/s11705-019-1828-x

COMMUNICATION

Synthesis and properties of water-soluble 1,9-dialkyl-substituted BF_2 azadipyrromethene fluorophores

Dan Wu, Gonzalo Durán-Sampedro, Donal F. O'Shea (✉)

Department of Chemistry, Royal College of Surgeons in Ireland (RCSI), Dublin 2, Ireland

Abstract Bis-alkylsulfonic acid and polyethylene glycol (PEG)-substituted BF_2 azadipyrromethenes have been synthesized by an adaptable and versatile route. Only four synthetic stages were required to produce the penultimate fluorophore compounds, containing either two alcohol or two terminal alkyne substituents. The final synthetic step introduced either sulfonic acid or polyethylene glycol groups to impart aqueous solubility. Sulfonic acid groups were introduced by reaction of the bis-alcohol-substituted fluorophore with sulfur trioxide, and a double Cu(I)-catalyzed cycloaddition reaction between the bis-alkyne fluorophore and methoxypolyethylene glycol azide yielded a neutral bis-pegylated derivative. Both fluorophores exhibited excellent near-infrared (NIR) photophysical properties in methanol and aqueous solutions. Live cell microscopy imaging revealed efficient uptake and intracellular labelling of cells for both fluorophores. Their simple synthesis, with potential for last-step structural modifications, makes the present NIR-active azadipyrromethene derivatives potentially useful as NIR fluorescence imaging probes for live cells.

Keywords NIR-fluorophores, live cell imaging, NIR-AZA

1 Introduction

Over the past decade, an increasing number of studies have focused on the development of near-infrared (NIR) chromophores, owing to their potential applications in numerous fields such as materials, assay development, *in vitro* and *in vivo* imaging, and medicine [1,2]. The NIR-active BF_2 azadipyrromethene (NIR-AZA) compounds are one such class of chromophores, which are being investigated for specific applications that range from solar cells to fluorescence-guided surgery [3]. In the earliest reports and subsequent studies, the substituent pattern contained four aryl groups at the 1-, 3-, 7-, and 9-positions of the NIR-AZA scaffold (compound **A** in Fig. 1) [4–7]. To date, this has been by far the most widely employed substitution pattern, although we later reported a synthetic route to derivatives in which the 1,9-diaryl groups were replaced with methyl substituents (**B**, Fig. 1) [8]. In the current work, we now expand the substituent pattern in **B** with a refined synthetic route to introduce 1,9-bis alkyl spacers containing water-solubilizing groups (WSGs) (Fig. 1). We are particular interested in further developing this substitution pattern, owing to the close match of the absorption and emission wavelengths with those of common fluorophores such as Alexa Fluor 647 and methylene blue [9,10]. We have previously shown that

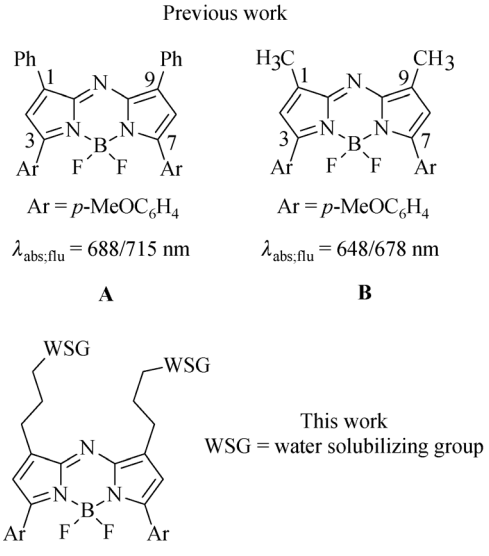

Fig. 1 Different substituent patterns and corresponding spectroscopic characteristics in $CHCl_3$ for NIR-AZA fluorophores.

Received December 19, 2018; accepted February 17, 2019

E-mail: donalfoshea@rcsi.ie

both polyethylene glycol (PEG)-substituted (pegylated) and alkyl-sulfonic acid groups successfully impart aqueous solubility to tetraaryl-substituted derivatives of type **A** [11−14].

2 Experimental

2.1 General procedures and materials

All reactions involving air-sensitive reagents were performed under nitrogen in oven-dried glassware, using the syringe-septum cap technique. All solvents were purified and degassed before use. Chromatographic separation was carried out under pressure on silica gel, using flash-column techniques. Reactions were monitored by thin-layer chromatography (TLC) carried out on 0.25 mm silica gel-coated aluminum plates, using UV light (254 nm) for visualization. Unless otherwise specified, all reagents were used as received without further purification. ^{1}H nuclear magnetic resonance (NMR) and ^{13}C NMR spectra were recorded at 400 and 100 MHz, respectively, and calibrated using residual non-deuterated solvent as an internal reference. Chemical shifts are reported in parts-per-million (ppm). Electrospray ionization (ESI) mass spectroscopy (MS) measurements were carried out using a microTOF-Q spectrometer in positive and negative modes, as required. High-performance liquid chromatography (HPLC) measurements were performed on a Shimadzu instrument equipped with a SPD-20AV Prominence UV-Vis detector. Separations were carried out using a Triart Phenyl 5 μm HPLC column (150 mm × 4.6 mm ID), with a water/CH_3CN solvent gradient. Fluorescence emission spectra were recorded on a Varian Cary Eclipse spectrophotometer, with excitation and emission slits of 5 nm. UV-Vis spectra were recorded on a Varian Cary 50 Scan spectrophotometer using quartz cuvettes of 1 cm path length.

2.2 Synthesis of **4a**

A solution of **2a** (3.5 g, 20 mmol) and phosphorane **3** (9.86 g, 24 mmol) in $CHCl_3$ (100 mL) was heated at reflux for 16 h under N_2. The mixture was cooled to room temperature (rt) and the solvent was removed in vacuo. The residue was purified by column chromatography (80:20 petroleum ether/EtOAc) to give **4a** (5.6 g, 18.4 mmol, 92%) as a yellow oil. ^{1}H NMR (400 MHz, $CDCl_3$): δ 7.93 (d, 2H, J = 8.9 Hz), 7.09–7.02 (m, 1H), 6.93–6.89 (m, 3H), 4.56 (t, 1H, J = 4.4 Hz), 3.85 (s, 3H), 3.84–3.76 (m, 2H), 3.50–3.40 (m, 2H), 2.43–2.38 (m, 2H), 1.86–1.77 (m, 3H), 1.74–1.65 (m, 1H), 1.59–1.48 (m, 4H) ppm. ^{13}C NMR (100 MHz, $CDCl_3$): δ 189.0, 163.3, 148.2, 130.8, 130.8, 125.8, 113.7, 99.0, 66.7, 62.4, 55.5, 30.7, 29.6, 28.4, 25.5, 19.6 ppm. MS (ESI): *m/z* $[M-H]^-$ calcd. for $C_{18}H_{23}O_4$ 303.16; found 303.41.

2.3 Synthesis of **4b**

A solution of **2b** (1.1 g, 8.7 mmol) and phosphorane **3a** (4.3 g, 10.44 mmol) in $CHCl_3$ (100 mL) was heated at reflux for 16 h under N_2. The mixture was cooled to rt and the solvent was then removed in vacuo. The residue was purified by column chromatography (80:20 petroleum ether/EtOAc) to give **4b** (2 g, 7.75 mmol, 89%) as a yellow oil. ^{1}H NMR (400 MHz, $CDCl_3$): δ 7.93 (d, J = 8.9 Hz, 2H), 7.07–6.97 (m, 1H), 6.95–6.87 (m, 3H), 4.13 (d, J = 2.4 Hz, 2H), 3.85 (s, 3H), 3.55 (t, J = 6.3 Hz, 2H), 2.45–2.35 (m, 3H), 1.87–1.75 (m, 2H) ppm. ^{13}C NMR (100 MHz, $CDCl_3$): δ 189.0, 163.4, 147.8, 130.9, 130.8, 126.0, 113.8, 79.9, 74.4, 69.1, 58.2, 55.5, 29.4, 28.2 ppm. MS (ESI): *m/z* $[M-H]^-$ calcd. $C_{16}H_{17}O_3$ 257.12; found 257.22.

2.4 Synthesis of **5a**

A solution of **4a** (5.6 g, 18.4 mmol) in ethanol (EtOH, 100 mL) was treated with nitromethane (10 mL, 184 mmol) and diethylamine (DEA, 8 mL, 77.3 mmol), followed by heating under reflux for 16 h. After allowing the reaction mixture to cool to rt, water (50 mL) was added and extracted with ethyl acetate (EtOAc, 3 × 50 mL). The combined organic layer was washed with brine, dried over Na_2SO_4, and the solvent was removed in vacuo. The residue was purified by column chromatography (80:20 petroleum ether/EtOAc) to give **5a** (6 g, 16.4 mmol, 89%) as an oil. ^{1}H NMR (400 MHz, $CDCl_3$): δ 7.93 (d, J = 8.9 Hz, 2H), 6.94 (d, J = 8.9 Hz, 2H), 4.65–4.50 (m, 3H), 3.87 (s, 3H), 3.86–3.63 (m, 3H), 3.52–3.46 (m, 1H), 3.42–3.35 (m, 1H), 3.19–3.01 (m, 2H), 2.94–2.85 (m, 1H), 1.84–1.73 (m, 1H), 1.72–1.66 (m, 3 H), 1.61–1.55 (m, 5H) ppm. ^{13}C NMR (100 MHz, $CDCl_3$): δ 196.6, 163.9, 130.5, 129.9, 114.0, 99.2, 78.8, 67.2, 62.6, 55.7, 39.5, 33.5, 30.8, 28.7, 27.1, 25.6, 19.8 ppm. MS (ESI): *m/z* $[M-H]^-$ calcd. for $C_{19}H_{26}NO_6$ 364.18; found 364.30.

2.5 Synthesis of **5b**

A solution of **4b** (1.5 g, 5.8 mmol) in EtOH (100 mL) was treated with nitromethane (3.2 mL, 58 mmol) and diethylamine (2.5 mL, 24.4 mmol), and then heated under reflux for 16 h. After allowing the reaction mixture to cool to rt, water (50 mL) was added and extracted with EtOAc (50 mL × 3). The combined organic layer was washed with brine, dried over Na_2SO_4, and the solvent was removed in vacuo. The residue was purified by column chromatography (80:20 petroleum ether/EtOAc) to give **5b** (1.6 g, 5.0 mmol, 85%) as an oil. ^{1}H NMR (400 MHz, $CDCl_3$): δ 7.93 (d, J = 8.9 Hz, 2H), 6.94 (d, J = 8.9 Hz, 2H), 4.55 (qd, J = 12.1, 5.8 Hz, 2H), 4.12 (d, J = 2.4 Hz, 2H), 3.87 (s, 3H), 3.52 (t, J = 6.1 Hz, 2H), 3.13 (dd, J = 17.6, 7.5 Hz, 1H), 3.02 (dd, J = 17.6, 5.4 Hz, 1H), 2.90–2.84 (m, 1H), 2.42 (t, J = 2.3 Hz, 1H), 1.71–1.66 (m, 2H),

1.60–1.55 (m, 2H) ppm. ^{13}C NMR (100 MHz, $CDCl_3$): δ 196.4, 163.8, 130.3, 129.7, 113.9, 79.7, 78.6, 74.4, 69.6, 58.2, 55.5, 39.3, 33.3, 28.4, 26.8 ppm. MS (ESI): *m/z* [M-H]$^-$ calcd. for $C_{17}H_{20}NO_5$ 318.13; found 318.42.

2.6 Synthesis of **1a**

A solution of **5a** (1 g, 2.7 mmol) and ammonium acetate (NH_4OAc, 7.3 g, 94.5 mmol) in methanol (MeOH, 50 mL) was heated under reflux for 9 h. The reaction mixture was allowed to cool to rt; then, water (100 mL) was added and the mixture was extracted with CH_2Cl_2 (100 mL × 2). The combined organic layer was washed with saturated $NaHCO_3$ (50 mL × 2) and water (50 mL), dried over Na_2SO_4, and the solvent was removed in vacuo. Without further purification, the isolated purple solid was dissolved in anhydrous CH_2Cl_2 (20 mL), treated with diisopropylethylamine (4.7 mL, 27 mmol) and boron trifluoride etherate ($BF_3 \cdot Et_2O$, 6 mL, 48.6 mmol), and then stirred for 2 h at rt under N_2. The residue was purified by flash chromatography on silica gel (9:1 petroleum ether/EtOAc) to afford **1a** (360 mg, 0.692 mmol, 26%) as a green metallic solid, m.p. 258°C–262°C. ^{1}H NMR (400 MHz, $CDCl_3$): δ 8.00 (d, J = 9.0 Hz, 4H), 6.94 (d, J = 9.0 Hz, 4H), 6.63 (s, 2H), 3.83 (s, 6H), 3.65 (t, J = 5.9 Hz, 4H), 2.83 (t, J = 7.2 Hz, 4H), 1.92–1.86 (m, 4H) ppm. ^{13}C NMR (100 MHz, $CDCl_3$): δ 162.0, 158.6, 146.6, 145.8, 131.7, 123.9, 121.3, 114.3, 60.8, 55.4, 33.0, 21.7ppm. ^{19}F NMR (376 MHz, $CDCl_3$): δ −132.78ppm. High-resolution MS (HRMS, ESI): *m/z* [M–H]$^-$calcd. for $C_{28}H_{29}BF_2N_3O_4$ 520.2225; found 520.2228.

2.7 Synthesis of **1b**

A solution of **5b** (1.5 g, 4.7 mmol) and NH_4OAc (13 g, 165 mmol) in MeOH (50 mL) was heated under reflux for 9 h. After allowing the reaction mixture to cool to rt, water (100 mL) was added and the mixture was extracted with CH_2Cl_2 (100 mL × 2). The combined organic layer was washed with saturated $NaHCO_3$ (50 mL × 2) and water (50 mL), dried over Na_2SO_4, and the solvent was removed in vacuo. Without further purification, the obtained purple solid was dissolved in anhydrous CH_2Cl_2 (50 mL), treated with diisopropylethylamine (8.2 mL, 47 mmol) and $BF_3 \cdot Et_2O$ (8.3 mL, 66 mmol) for 2 h at room temperature under N_2. The residue was then purified by flash chromatography on silica gel (9:1 petroleum ether/EtOAc) to afford **1b** (0.88 g, 1.48 mmol, 31%) as a green metallic solid, m.p. 142°C–144°C. ^{1}H NMR (400 MHz, $CDCl_3$): δ 8.01 (d, J = 9.0 Hz, 4H), 6.96 (d, J = 9.0 Hz, 4H), 6.63 (s, 2H), 4.18 (d, J = 2.4 Hz, 4H), 3.85 (s, 6H), 3.62 (t, J = 6.3 Hz, 4H), 2.85 (t, J = 7.5 Hz, 4H), 2.44 (t, J = 2.4 Hz, 2H), 2.05–1.98 (m, 4H) ppm. ^{13}C NMR (100 MHz, $CDCl_3$): δ 161.8, 158.1, 147.0, 145.8, 131.6, 124.2, 120.7, 114.2, 80.0, 74.4, 69.4, 58.2, 55.5, 29.7, 22.6 ppm. ^{19}F NMR (376 MHz, $CDCl_3$): δ − 133.01 ppm. HRMS (ESI): *m/z* [M-H]$^-$ calcd. for $C_{34}H_{33}BF_2N_3O_4$ 596.2532; found 596.2541.

2.8 Synthesis of **6a**

A solution of **1a** (60 mg, 0.12 mmol) and sulfur trioxide trimethylamine complex ($SO_3 \cdot NMe_3$, 96 mg, 0.69 mmol, 6 equiv.) in anhydrous tetrahydrofuran (THF, 5 mL) was stirred under reflux for 1 h. Once TLC indicated complete consumption of the starting material, the reaction mixture was allowed to cool to rt, the solvent was evaporated in vacuo, and the crude material was purified by a Sephadex G-25 column eluted with HPLC-grade water. The pure fractions were combined and the solvent was removed by freeze-drying to give **6a** (84 mg, 92%) as a green metallic solid, m.p. > 250°C. ^{1}H NMR (400 MHz, deuterated dimethyl sulfoxide (DMSO-d_6)): δ 8.08 (d, J = 8.9 Hz, 4H), 7.10 (d, J = 8.9 Hz, 4H), 7.08 (s, 2H), 3.87 (s, 6H), 3.83 (t, J = 6.3 Hz, 4H), 2.79–2.78 (m, 22H), 1.98–1.91 (m, 4H) ppm. ^{13}C NMR (100 MHz, DMSO-d_6): δ 162.2, 157.8, 147.0, 145.4, 132.0, 123.7, 121.9, 114.9, 65.5, 56.0, 44.6, 29.2, 22.4 ppm. ^{19}F NMR (376 MHz, DMSO-d_6): δ − 131.40 ppm.

2.9 Synthesis of **6b**

A solution of **1b** (10 mg, 0.02 mmol) and methoxypolyethylene glycol azide with PEG average M_n = 1000 (azide-PEG_{1000}, 40 mg, 0.04 mmol) in THF/H_2O (2:1, 1 mL) was treated with a 250 mg/mL aqueous solution of $CuSO_4 \cdot 5H_2O$ (20 μL, 5 mg, 0.02 mmol) and ascorbic acid (7 mg, 0.04 equiv.), and the mixture was stirred for 2 h at rt under N_2. After purifying the mixture by a Sephadex G-25 column eluted with water to remove salts, the purification was completed by reverse-phase preparative HPLC (CH_3CN/H_2O = 70:30). The pure fractions were combined and the solvent was removed by freeze-drying to give **6b** as a deep green solid (31 mg, 71%), m.p. 50°C–52°C.

2.10 Cell culture

HeLa-Kyoto cells were seeded at a density of 1 × 10^4 cells per well on an eight-well removable chamber slide (Millipore) or a glass-bottom chamber slide (Ibidi), and allowed to proliferate for 24 h at 5.0% CO_2 and 37°C. Cells were cultured in Dulbecco's modified Eagle's medium (DMEM) supplemented with 10% fetal bovine serum (FBS), 1% penicillin/streptomyosin, and 1% L-glutamate.

2.11 Live-cell imaging

HeLa-Kyoto cells were seeded at a density of 1 × 10^4 cells per well on a glass-bottom chamber slide (Ibidi) and allowed to proliferate for 24 h at 5% CO_2 and 37°C. Cells were cultured in DMEM supplemented with 10% FBS, 1% penicillin/streptomyosin, and 1% L-glutamate. The slides

were placed on the microscope stage surrounded by an incubator to maintain the temperature at 37°C and the CO_2 levels at 5%. Solutions (10 μL) of **6a** and **6b** (100 μmol/L) in sterile PBS were added to 190 μL of DMEM to afford final **6a** and **6b** concentrations of 5 μmol/L. The cell medium was replaced with these solutions and the cells were imaged at 30, 60, 90, and 120 min time points. After each time point, the cell medium was removed from the well; the cells were then washed three times with pre-warmed PBS (37°C) and replaced by fresh medium. Differential interference contrast (DIC) imaging was used to select a field of view and focus on a group of cells. DIC and fluorescence images were acquired on an Olympus IX73 epifluorescence microscope fitted with an Andor iXon Ultra 888 electron multiplying charge-coupled device (EMCCD), using a 60×/1.42 oil PlanApo objective (Olympus). Z-stacks with 27 optical slices spaced 0.5 μm apart were acquired in the NIR channels. The excitation and emission filters used for the NIR imaging were 640 (14) and 705 (72) nm, respectively, with 50 ms exposure.

3 Results and discussion

For this work, we selected two target NIR-AZA derivatives bearing 1,9-bis(propan-1-ol) (**1a**) or 1,9-bis(3-(prop-2-yn-1-yloxy)propyl) (**1b**) groups, from which water-soluble derivatives were expected to be readily accessible (Fig. 2).

The synthesis started with the preparation of the 4-(allyloxy)butanal (**2a**) and 4-((tetrahydro-2*H*-pyran-2-yl)oxy)butanal (**2b**) aldehydes, which was achieved following literature procedures [15,16]. Next, the Wittig reaction of **2a** and **2b** with 1-(4-methoxyphenyl)-2-(triphenylphosphanylidene)ethan-1-one (**3**) in chloroform under reflux readily provided the *α*,*β*-unsaturated ketones **4a** and **4b**, respectively (Scheme 1). The 1,4-conjugate addition of nitromethane to **4a** and **4b** in EtOH in the presence of DEA gave the nitro ketones **5a** and **5b**, respectively in high yield.

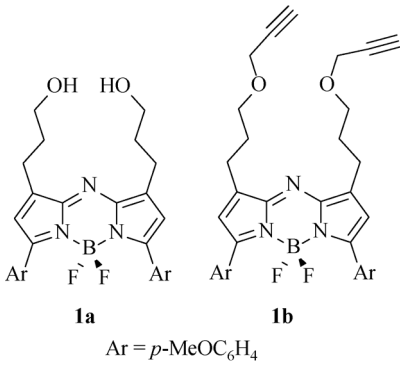

Fig. 2 *Bis*-alcohol and *bis*-alkyne substituted NIR-AZA targets **1a** and **1b**.

Subsequent treatment with NH_4OAc in methanol under reflux gave the substituted azadipyrromethene; *in situ* conversion to the corresponding BF_2 chelates **1a** and **1b** was achieved using BF_3 etherate and *N*,*N*-diisopropylethylamine (DIPEA) in CH_2Cl_2 at rt (Scheme 2). In the case of the derivative **5a**, tetrahydropyran (THP) deprotection occurred *in situ*, presumably due to the action of the excess BF_3 etherate, yielding the desired bis-alcohol fluorophore product **1a**.

The **1a** and **1b** compounds exhibited the expected spectroscopic properties in chloroform and methanol organic solvents, with absorbance and emission maxima

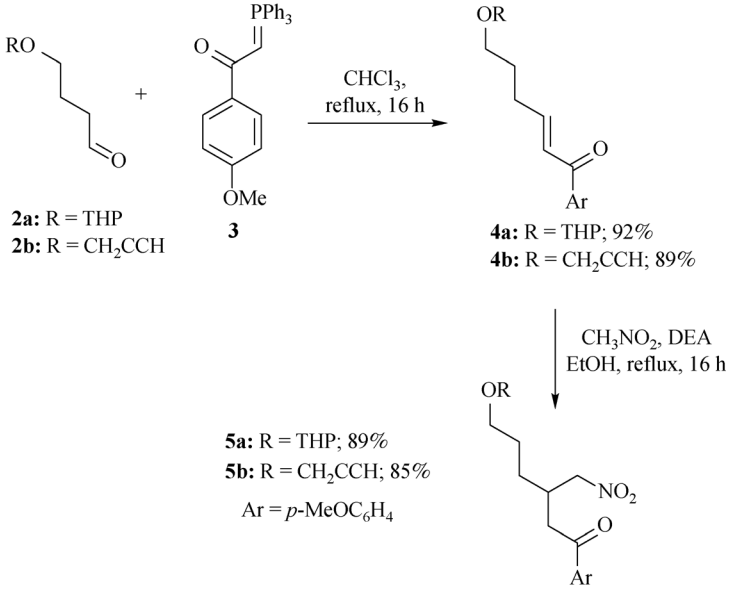

Scheme 1 Synthesis of azadipyrromethene precursors.

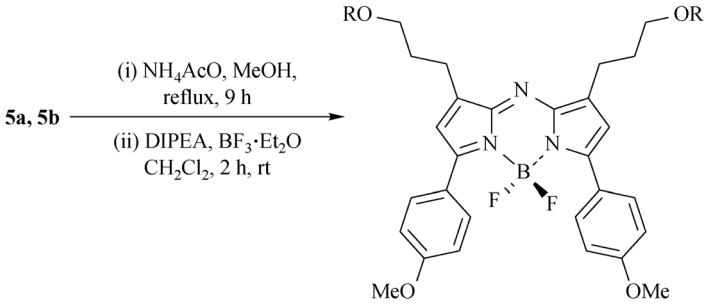

1a: R = H; 26%
1b: R = CH_2CCH; 31%

Scheme 2 Synthesis of NIR-AZA fluorophores **1a** and **1b.**

Table 1 Spectroscopic properties of **1a** and **1b** compounds

NIR-AZA	$\lambda_{abs,max}$ /nm $CHCl_3$ (MeOH)	$\lambda_{flu,max}$ /nm $CHCl_3$ (MeOH)	Φ_f[a)] $CHCl_3$ (MeOH)
1a	660 (650)	695 (678)	0.27 (0.14)
1b	653 (651)	680 (677)	0.21 (0.16)

a) Methylene blue (MB) (Φ = 0.03 in MeOH) was used as standard [9]

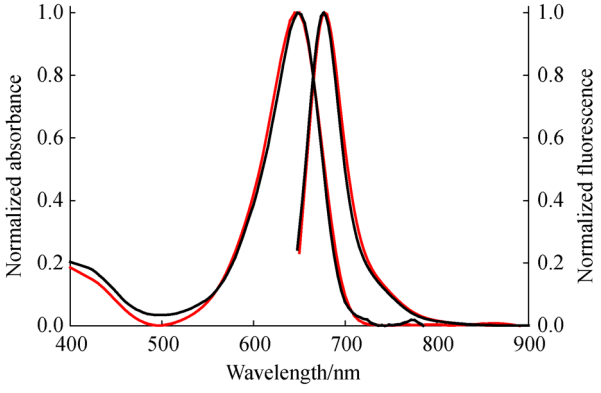

Fig. 3 Absorption and emission spectra of **1a** (red) and **1b** (black) at a concentration of 5 μmol/L.

at 650−660 and 677−695 nm, respectively (Table 1, Fig. 3). Slight differences were noted between $CHCl_3$ and MeOH, with the protic solvent causing minor hypsochromic shifts. Interestingly, high fluorescent quantum yields (Φ_f) were obtained in both solvents.

To complete the new substitution pattern presented in this work, **1a** was converted to the water-solube derivative **6a** by reaction with $SO_3 \cdot NMe_3$ under reflux in THF for 1 h (Scheme 3). The product was isolated and purified using a Sephadex G-25 column. Next, the double cycloaddition click reactions of **1b** with azide-PEG_{1000} in the presence of $CuSO_4$/ascorbic acid at rt completed the alternative route to include water-solubilizing groups (Scheme 3).

Encouragingly, we found that both **6a** and **6b** were readily soluble in water and phosphate buffered saline (PBS); this allowed their spectroscopic characteristics to be determined based on the spectroscopy behavior recorded in PBS, DMEM, and methanol (Table 2, Fig. 4). The UV-Vis/fluorescence spectra of **6a** and **6b** in aqueous media showed little difference from each other, as well as higher quantum yields compared with MB.

In addition, the absorption and emission wavelengths of **6a** and **6b** closely matched those of MB, which further confirms the versatility of the new synthetic protocol developed in this work. This is particularly encouraging for more advanced uses of water-soluble NIR-AZA derivatives with this substitution pattern, as recent clinical trial studies have reported the use of MB as imaging agent for fluorescence-guided surgery [17–19].

Encouraged by their excellent properties in aqueous solutions, we investigated the potential use of doubly negative-charged **6a** and neutral **6b** for live-cell fluorescence imaging. Using HeLa-Kyoto cancer cells as a test line, efficient cell uptake was observed for both fluorophores within 30 min, with the fluorescence intensity continuously increasing up to 120 min of incubation (cf. Electronic Supplementary Material, ESM). Representative images taken following 60 min of incubation are shown in Fig. 5. Similar cell staining patterns were observed for **6a** and **6b**, with a mixture of punctate vesicles and more diffuse fluorescent areas. Z-stack acquisition of multiple focal planes through individual cells clearly showed that fluorophore internalization had occurred (cf. ESM). In addition, images continuously acquired every 10 s showed bright fluorescent vesicles in motion through the cytoplasm, whose movements could be tracked over prolonged time periods (cf. ESM). Taken together, these results prove

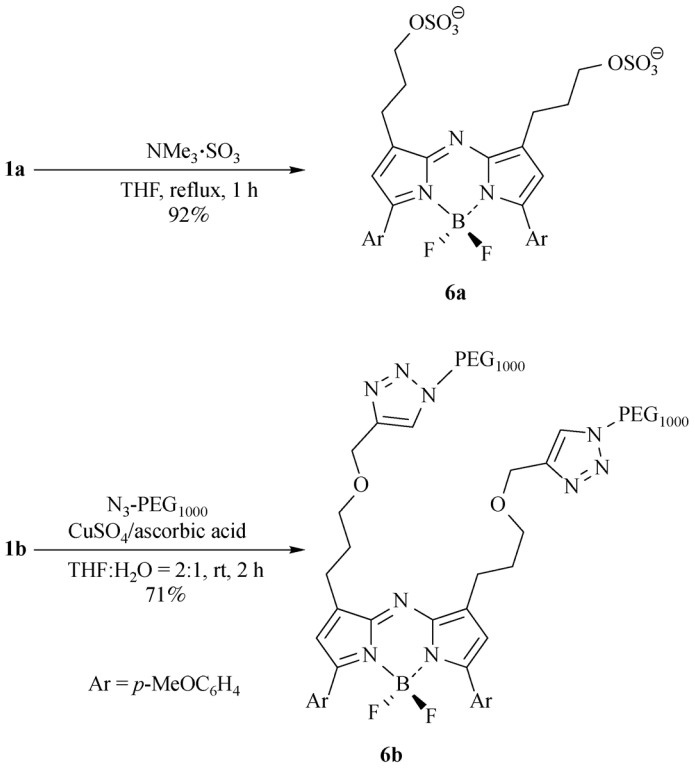

Scheme 3 Synthesis of water-soluble NIR-AZA derivatives.

Table 2 Spectroscopic properties of **6a**, **6b**, and MB[a)]

Fluorophore	Solvent	$\lambda_{abs,\ max}$ /nm	$\lambda_{flu,\ max}$ /nm	Φ_f
MB	PBS	670	690	0.01
6a	MeOH	650	675	0.12
6a	PBS	651	690	0.03
6a	DMEM	651	691	0.03
6b	MeOH	651	679	0.12
6b	PBS	657	694	0.06
6b	DMEM	658	694	0.05

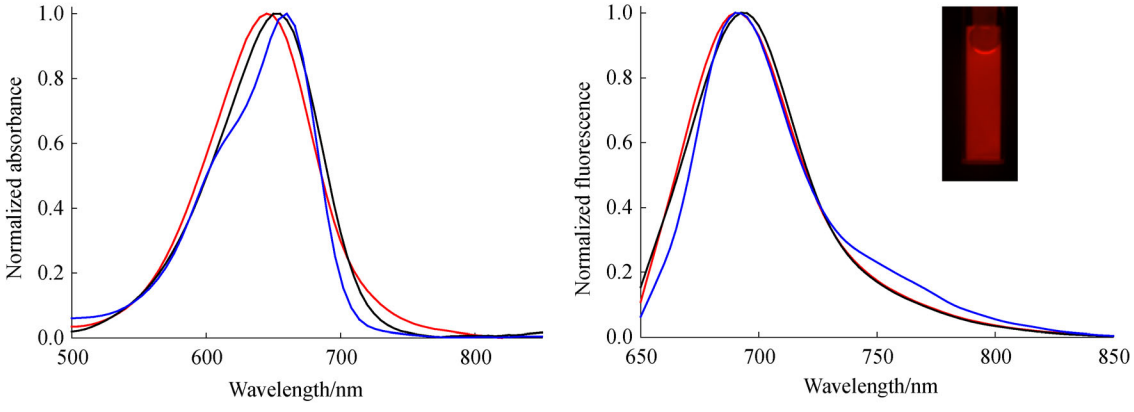

Fig. 4 Absorption and emission spectra of **6a** (red), **6b** (black), and MB (blue) in PBS at a concentration of 5 μmol/L. Inset: Emission image of cuvette containing **6a** in PBS.

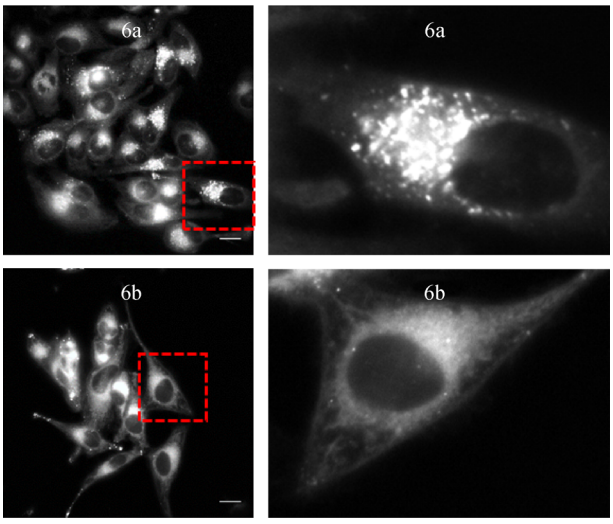

Fig. 5 Widefield microscopy images of live HeLa cells upon incubation with **6a** and **6b** for 1 h. Top: fluorescence images of cells stained with **6a** (5 μmol/L); Bottom: fluorescence images of **6b** (5 μmol/L) in HeLa cells. The right panels in each row display enlargements of the areas within the red boxes shown in the left panels. Scale bars = 20 μm.

that both bis-sulfonic acid and bis-PEG solubilizing groups can be employed to facilitate cell delivery by the fluorophores.

4 Conclusions

In summary, we developed an efficient and adaptable four-step synthesis of a new substitution pattern for the NIR-AZA fluorophore class, which allows water-soluble groups to be incorporated as the last step of the synthesis. The absorption and emission spectral properties of these systems in aqueous media highlight their promising potential for live-cell imaging and *in vivo* biomedical applications.

Acknowledgements This work is supported by the European Union's Horizon 2020 research and innovation program, under the Marie-Sklodowska-Curie grant agreement No. 707618. DOS declares the following competing financial interest: patents have been filed on BF_2-azadipyrromethene-based NIR fluorophores (EP2493898 and US8907107).

Electronic Supplementary Material Supplementary material is available in the online version of this article at https://doi.org/10.1007/s11705-019-1828-x and is accessible for authorized users.

References

1. Yuan L, Lin W, Zheng K, He L, Huang W. Far-red to near infrared analyte-responsive fluorescent probes based on organic fluorophore platforms for fluorescence imaging. Chemical Society Reviews, 2013, 42(2): 622–661
2. Pansare V J, Hejazi S, Faenza W J, Prud'homme R K. Review of long-wavelength optical and NIR imaging materials: Contrast agents, fluorophores and multifunctional nano carriers. Chemistry of Materials, 2012, 24(5): 812–827
3. Ge Y, O'Shea D F. Azadipyrromethenes: From traditional dye chemistry to leading edge applications. Chemical Society Reviews, 2016, 45(14): 3846–3864
4. Killoran J, Allen L, Gallagher J F, Gallagher W M, O'Shea D F. Synthesis of BF_2 chelates of tetraarylazadipyrromethenes and evidence for their photodynamic therapeutic behavior. Chemical Communications, 2002, 17: 1862–1863
5. Grossi M, Palma A, McDonnell S O, Hall M J, Rai D K, Muldoon J, O'Shea D F. Mechanistic insight into the formation of tetraarylazadipyrromethenes. Journal of Organic Chemistry, 2012, 77(20): 9304–9312
6. O'Connor A E, Mc Gee M M, Likar Y, Ponomarev V, Callanan J J, O'Shea D F, Byrne A T, Gallagher W M. Mechanism of cell death mediated by a BF_2-chelated tetraaryl-azadipyrromethene photodynamic therapeutic: Dissection of the apoptotic pathway *in vitro* and *in vivo*. International Journal of Cancer, 2012, 130(3): 705–715
7. Cheung S, O'Shea D F. Directed self-assembly of fluorescence responsive nanoparticles and their use for real-time surface and cellular imaging. Nature Communications, 2017, 8(1): 1885
8. Wu D, O'Shea D F. Synthesis and properties of BF_2-3,3′-dimethyldiarylazadipyrromethene near-infrared fluorophores. Organic Letters, 2013, 15(13): 3392–3395
9. Olmsted J. Calorimetric determinations of absolute fluorescence quantum yields. Journal of Physical Chemistry, 1979, 83(20): 2581–2584
10. Berlier J E, Rothe A, Buller G, Bradford J, Gray D R, Filanoski B J, Telford W G, Yue S, Liu J, Cheung C Y, et al. Quantitative comparison of long-wavelength alexa fluor dyes to cy dyes: Fluorescence of the dyes and their bioconjugates. Journal of Histochemistry and Cytochemistry, 2003, 51(12): 1699–1712
11. Wu D, Cheung S, Sampedro G, Chen Z L, Cahill R A, O'Shea D F. A DIE responsive NIR-fluorescent cell membrane probe. Biochimica et Biophysica Acta–Biomembranes, 2018, 1860(11): 2272–2280
12. Wu D, Daly H C, Conroy E, Li B, Gallagher W M, Cahill R A, O'Shea D F. PEGylated BF_2-Azadipyrromethene (NIR-AZA) fluorophores, for intraoperative imaging. European Journal of Medicinal Chemistry, 2019, 161: 343–353
13. Daly H C, Sampedro G, Bon C, Wu D, Ismail G, Cahill R A, O'Shea D F. BF_2-azadipyrromethene NIR-emissive fluorophores with research and clinical potential. European Journal of Medicinal Chemistry, 2017, 135: 392–400
14. Monopoli M P, Zendrini A, Wu D, Cheung S, Sampedro G, Ffrench B, Nolan J, Piskareva O, Stalings R L, Ducoli S, et al. Endogenous exosome labelling with an amphiphilic NIR-fluorescent probe. Chemical Communications, 2018, 54(52): 7219–7222
15. Denney D B, Smith L C, Song J, Rossi C J, Hall C D. Reactions of phosphoranes with peracids. Journal of Organic Chemistry, 1963, 28 (3): 778–780
16. Yamamoto Y, Kurihara K, Yamada A, Takahashi M, Takahashi Y, Miyaura N. Intramolecular allylboration of γ-(ω-formylalkoxy)

allylboronates for syntheses of *trans*- or *cis*-2-(ethenyl)tetrahydropyran-3-ol and 2-(ethenyl)oxepan-3-ol. Tetrahedron, 2003, 59(4): 537–542

17. Verbeek F P, van der Vorst J R, Schaafsma B E, Swijnenburg R J, Gaarenstroom K N, Elzevier H W, van de Velde C J, Frangioni J V, Vahrmeijer A L. Intraoperative near infrared fluorescence guided identification of the ureters using low dose methylene blue: A first in human experience. Journal of Urology, 2013, 190(2): 574–579
18. Al-Taher M, van den Bos J, Schols R M, Bouvy N D, Stassen L P. Fluorescence ureteral visualization in human laparoscopic colorectal surgery using methylene blue. Journal of Laparoendoscopic & Advanced Surgical Techniques. Part A., 2016, 26(11): 870–875
19. Matsui A, Tanaka E, Choi H S, Kianzad V, Gioux S, Lomnes S J, Frangioni J V. Real-time, near-infrared, fluorescence-guided identification of the ureters using methylene blue. Surgery, 2010, 148(1): 78–86